Fluorescence Lifetime Resolution of Spectra in the Frequency Domain Using Multiway Analysis

David W. Millican and Linda B. McGown*

Department of Chemistry, P. M. Gross Chemical Laboratory, Duke University, Durham, North Carolina 27706

Spectral resolution of two-component systems by multiway analysis of excitation–emission–frequency arrays is compared with single-matrix analysis of steady-state excitation–emission matrices for both real and computer-simulated systems. Fluorescence lifetime selectivity can improve resolution, especially for the minor component in mixtures in which the two components have unequal contributions to the total intensity. However, in some cases the lifetime difference between two fluorophores is insufficient to aid resolution.

INTRODUCTION

The resolution of the fluorescence spectra of individual components from multicomponent excitation–emission matrices (EEMs) by chemometric methods has been extensively studied (*1*). Previous work has demonstrated the use of fluorescence lifetime selectivity to facilitate spectral resolution for two-component systems in both the time domain (*2–4*) and frequency domain (*5*). In the latter studies, we demonstrated the enhancement of spectral resolution by phase-resolved fluorescence spectroscopy (PRFS), in which the phase-resolved fluorescence intensity (PRFI) is collected as a function of both excitation and emission wavelength at a given modulation frequency to generate a phase-resolved EEM (PREEM). Since the PRFI of long-lived fluorophores is relatively enhanced at low modulation frequencies and the PRFI of short-lived fluorophores is relatively enhanced at higher frequencies, resolution of a particular component can be improved by collecting the PREEM at a modulation frequency favorable to that component.

We have recently described an extension of the PREEM approach in which we simultaneously analyze a stack of three PREEMs, each collected at a different modulation frequency (*6*). Analysis of this three-way excitation–emission–frequency array (EEFA) by multiway decomposition techniques was shown to be effective for resolving an approximately equal-intensity mixture of benzo[*k*]fluoranthene (BkF) and benzo[*b*]fluoranthene (BbF). In this paper, we describe the results of the EEFA approach for the analysis of several two-component mixtures in which the relative intensity contributions of the components were varied. The two-component systems were chosen to give varying degrees of spectral overlap and lifetime similarity. Simulations of two-component mixtures were used together with the real mixtures to explore the effects of spectral overlap, lifetime difference, and noise level, in order to better understand both the advantages and limitations of the EEFA approach relative to single-matrix EEM and PREEM techniques.

THEORY

The principles of PFRS have been thoroughly documented (*7, 8*) and will be only briefly discussed here. In PRFS, the sample is excited with sinusoidally modulated light, resulting in fluorescence emission that is modulated at the same frequency, but phase-shifted and demodulated relative to the excitation, to an extent determined by the fluorescence lifetime, τ. Phase-sensitive detection of the modulated (ac) component of the fluorescence signal produces the time-independent PRFI given by (*9*)

$$\mathrm{PRFI} = A' m_{ex} \frac{\cos(\phi_D - \arctan(\omega\tau))}{((\omega\tau)^2 + 1)^{1/2}} \quad (1)$$

where A' is the steady-state (dc) fluorescence intensity, m_{ex} is the modulation depth (ac/dc ratio) of the exciting light, ω is the angular modulation frequency (that is, 2π times the linear modulation frequency f), and ϕ_D is the detector phase angle, which can be set to any value between 0° and 360°. The PRFI is also a function of the spectral characteristics and concentration of the component, through the steady-state intensity A'.

Since PRFIs of independent emitters in a mixture are additive, the total PREEM for a multicomponent sample at a given ϕ_D and ω is the sum of the PREEMs of the independently emitting components. For a two-component PREEM composed of m emission spectra of n points each

$$\mathbf{M} = a_1\mathbf{C}_1 + a_2\mathbf{C}_2 \quad (2)$$

where $\mathbf{M}$ is the $m \times n$ PREEM of the mixture, a_1 and a_2 are scalars reflecting the relative contributions of the two components, and $\mathbf{C}_1$ and $\mathbf{C}_2$ are the normalized $m \times n$ PREEMs of the individual components. The PREEMs of the individual components can, in the absence of noise, be described as the product of the excitation and emission spectral vectors of the component

$$\mathbf{C}_i = \mathbf{x}_i(\mathbf{y}_i)^T \quad (3)$$

where $\mathbf{x}_i$ is the $m \times 1$ excitation vector and $\mathbf{y}_i$ is the $n \times 1$ emission vector of the ith component. $\mathbf{M}$ can therefore be described by

$$\mathbf{M} = \mathbf{X}\mathbf{D}_a\mathbf{Y}^T \quad (4)$$

where $\mathbf{X}$ is an $m \times 2$ matrix whose columns are x_1 and x_2, $\mathbf{Y}$ is an $n \times 2$ matrix whose columns are y_1 and y_2, and $\mathbf{D}_a$ is a 2×2 diagonal matrix whose elements are a_1 and a_2.

In contrast to noise-free data matrix, the rank of a real data matrix containing noise will usually not be equal to the number of components contributing to the signal. However, the noise-free case can be approximated by the first k terms of the singular value decomposition (SVD) of $\mathbf{M}$, where k is the number of noninteracting fluorophores. For the two-component case

$$\mathbf{M} = \sigma_1\mathbf{u}_1\mathbf{v}_1^T + \sigma_2\mathbf{u}_2\mathbf{v}_2^T \quad (5)$$

where σ_1^2 and σ_2^2 are the largest two eigenvalues of $\mathbf{M}\mathbf{M}^T$ or $\mathbf{M}^T\mathbf{M}$, $\mathbf{u}_1$ and $\mathbf{u}_2$ are the corresponding eigenvectors of $\mathbf{M}\mathbf{M}^T$, and $\mathbf{v}_1$ and $\mathbf{v}_2$ are the corresponding eigenvectors of $\mathbf{M}^T\mathbf{M}$. $\mathbf{M}$ can then be expressed in a manner analogous to eq 4 as

$$\mathbf{M} = \mathbf{U}\mathbf{D}_\sigma\mathbf{V}^T \quad (6)$$

Comparing eqs 4 and 6, we can normalize $\mathbf{X}$, $\mathbf{Y}$, $\mathbf{U}$, and $\mathbf{V}$ such that

$$\mathbf{X}\mathbf{Y}^T = \mathbf{U}\mathbf{V}^T \quad (7)$$

There must then exist some transformation between the row

0003-2700/90/0362-2242$02.50/0

and column spaces **U** and **V**, which can be mathematically derived, and the excitation and emission spectral vectors in **X** and **Y**, which are the objectives in spectral resolution.

Wavelength Component Vectorgram (WCV) Analysis (10). In this single-matrix analysis, the desired transformation is a 2 × 2 matrix **K** where

$$\mathbf{X} = \mathbf{UK} \tag{8}$$

and

$$\mathbf{Y} = \mathbf{V}(\mathbf{K}^{\mathrm{T}})^{-1} \tag{9}$$

To fine **K**, we impose the constraints of nonnegativity upon the intensities of the resolved spectra and unit magnitude upon the columns of **K**. This allows **K** to be parameterized as

$$k_{11} = \cos\theta_1 \quad k_{12} = \cos\theta_2$$
$$k_{21} = \sin\theta_1 \quad k_{22} = \sin\theta_2 \tag{10}$$

A range of possible solutions is found by transforming **U** and **V** into polar coordinates and finding values for θ which satisfy eqs 8 and 9 and the stated constraints.

Multiway Analysis (6). Here, **M** represents an EEFA comprised of the individual PREEMs, represented as $\mathbf{M}_f$ where the subscript f refers to the modulation frequency at which the PREEM was collected. Each $\mathbf{M}_f$ is given as

$$\mathbf{M}_f = \mathbf{XD}_f\mathbf{Y}^{\mathrm{T}} \tag{11}$$

where **X** and **Y** are given by eq 4 and $\mathbf{D}_f$ is a diagonal matrix whose elements reflect the relative contributions of the individual components. **M** is decomposed to find a basis for the row and column space common between the layers of the EEFA

$$\mathbf{M}_f = \mathbf{UC}_f\mathbf{V}^{\mathrm{T}} \tag{12}$$

where **U** and **V** are matrices whose columns are bases for the common column and row spaces, respectively, and

$$\mathbf{C}_f = (\mathbf{U}^{\mathrm{T}}\mathbf{U})^{-1}\mathbf{U}^{\mathrm{T}}\mathbf{M}_f\mathbf{V}(\mathbf{V}^{\mathrm{T}}\mathbf{V})^{-1} \tag{13}$$

The transformation matrices **P** and **Q** such that

$$\mathbf{X} = \mathbf{UP}$$

and

$$\mathbf{Y} = \mathbf{VQ}$$

are found by diagonalizing any two $\mathbf{C}_f$s

$$\mathbf{P}^{-1}\mathbf{C}_i\mathbf{C}_j^{-1}\mathbf{P} = \mathbf{D}_i\mathbf{D}_j^{-1}$$

$$\mathbf{Q}^{\mathrm{T}}\mathbf{C}_i^{-1}\mathbf{C}_j(\mathbf{Q}^{\mathrm{T}})^{-1} = \mathbf{D}_i^{-1}\mathbf{D}_j \tag{15}$$

EXPERIMENTAL SECTION

PAH Data. Solutions of BkF (Accustandard, New Haven, CT) and BbF (Analabs, North Haven, CT) were prepared as previously described (*5*). Solutions of anthracene (ANT) (Ultra Scientific, North Kingstown, RI), 9,10-diphenylanthracene (DPA) (Aldrich, Milwaukee, WI), and 1,3,6,8-tetraphenylpyrene (TPP) (Pfaltz & Bauer, Waterbury, CT) were prepared in absolute ethanol. Five mixtures were prepared for each two-component system to obtain a range of steady-state intensity ratios, with individual component concentrations ranging from 0.3 to 5.0 μM.

Fluorescence measurements of the B(k)F/B(b)F system were made with an SLM 4800S phase modulation spectrofluorometer (SLM Instruments, Urbana, IL) as previously described (*5*). Fluorescence measurements of the DPA/ANT and DPA/TPP systems were made with an SLM 48000S multifrequency phase modulation spectrofluorometer. Solutions were measured in quartz cuvettes at 25.0 ± 0.1 °C and were not deoxygenated. Steady-state EEMs and PREEMs were collected at 5, 10, 20, 40, and 80 MHz for DPA/ANT and 10, 20, 40, 80, 120, and 160 MHz for DPA/TTP. All EEMs and PREEMs were collected in a ratiometric mode as a series of emission spectra, with 4-nm intervals for both emission and excitation wavelengths. Each intensity is the mean of 10 measurements, collected over a period of 3 s and internally averaged by the instrument electronics. Scattered light was suppressed in each PREEM by adjusting the detector phase angle to null the scattered light signal from a solution of kaolin in water for each modulation frequency.

Synthetic Data. Simulated EEMs and PREEMs were generated from unit-intensity Gaussian curves of varying degrees of overlap. In a simulated EEFA, each synthetic peak was assigned a lifetime and varied in intensity according to

$$I = \frac{\cos(\phi_{\mathrm{D}} - \arctan(\omega\tau))}{((\omega\tau)^2 + 1)^{1/2}} \tag{16}$$

where I is the relative intensity of the Gaussian function. The shapes of the simulated spectra were varied by multiplication with a sine function and addition to the unperturbed function, in order to place the resulting split in the peak above baseline. Noise was added to the synthetic EEMs and PREEMs using

$$I' = I + rI^{1/2}f_{\mathrm{rand}} \tag{17}$$

where I' is the new noise-modified data, f_{rand} is the output of a random number generator with a mean of 0 and unit variance, and r is a factor introduced to vary the noise contribution (for example, r = 0.10 yields a peak signal-to-noise ratio of 10:1 and r = 0.25 yields a peak signal-to-noise ratio of 4:1).

Data Analysis. WCV analysis was carried out with previously described algorithms (*10*) on a Hewlett-Packard 9920U microcomputer. Multiway analysis was performed on an IBM PC/AT using routines written in MATLAB (The Mathworks, South Natick, MA) that were based on algorithms previously described (*6*). Contour plots were also prepared on an IBM PC/AT using SURFER software (Golden Software, Golden, CO).

RESULTS AND DISCUSSION

The modulation frequency responses of the PAHs making up the three two-component systems are shown in Figure 1, and their steady-state EEMs are shown in Figure 2. BkF and BbF have moderately overlapping EEMs (uncorrected matrix correlation (UMC) (*10*) for BkF and BbF = 0.3413) and very different fluorescence lifetimes (29 ns for BbF and 8 ns for BkF). DPA and ANT are more highly overlapped (UMC for DPA and ANT = 0.5036) and have much more similar lifetimes (DPA τ = 6 ns and ANT τ = 4 ns). DPA and TPP are even more highly overlapped than DPA and ANT (UMC for DPA and TPP = 0.9145) but have a greater difference in their fluorescence lifetimes (TPP τ = 2.5 ns).

Selection of Modulation Frequencies. The BkF–BbF system was measured at the three frequencies available on the SLM 4800S (6, 18, and 30 MHz). The DPA–ANT and DPA–TPP systems were measured on the multifrequency SLM 48000S, which provides essentially continuous frequency selection between 1 and 250 MHz. The five frequencies used for DPA–ANT and the six used for DPA–TPP were chosen to provide good coverage of the frequency response ranges shown in Figure 1.

BkF and BbF. The UMCs are shown in Table I for the component spectra extracted from this system by multiway analysis of PREEM data and WCV analysis of steady-state data with the component spectra obtained directly from standard solutions of the individual components. It is interesting to note that while resolution of the major component of an unequal mixture is generally not significantly improved by multiway lifetime selectivity (and is actually degraded in the 10:1 BkF–BbF mixture), resolution of the minor component is always enhanced. In addition, although our previous work (*5*) showed that enhanced resolution of a particular component is also obtained by WCV analysis of individual PREEMs collected at a frequency favorable to that component, greater enhancement is obtained by combining the individual PREEMs in the multiway analysis.

DPA and ANT. Since the components of this system have more highly overlapping spectra and more similar lifetimes than BkF and BbF, it is more difficult to resolve, as is shown

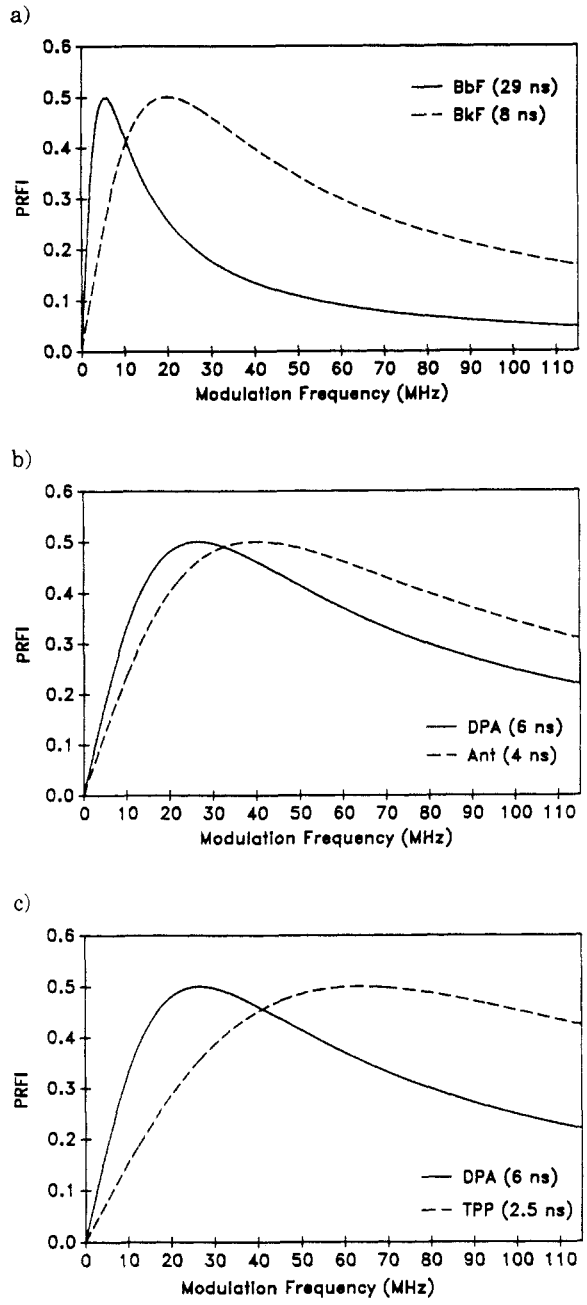

Figure 1. Theoretical plots of PRFI vs modulation frequency for (a) BbF and BkF, (b) DPA and ANT, and (c) DPA and TPP.

Table I. UMCs of Extracted Component Spectra of BkF and BbF from Multiway Analysis Using 6-, 18-, and 30-MHz PREEMs and WCV Analysis

	extracted EEM 1		extracted EEM 2	
	BkF	BbF	BkF	BbF
5:1 BkF–BbF				
PREEM Multiway	0.9837	0.3587	0.3607	0.9979
steady-state WCV	0.9780	0.3136	0.5425	0.9595
1:5 BkF–BbF				
PREEM Multiway	0.9839	0.3365	0.3634	0.9982
steady-state WCV	0.9465	0.1566	0.3716	0.9974
10:1 BkF–BbF				
PREEM multiway	0.9836	0.3694	0.3219	0.9975
steady-state WCV	0.9941	0.3616	0.4330	0.9257
1:10 BkF–BbF				
PREEM multiway	0.9812	0.3541	0.3565	0.9982
steady-state WCV	0.9444	0.1491	0.3602	0.9988

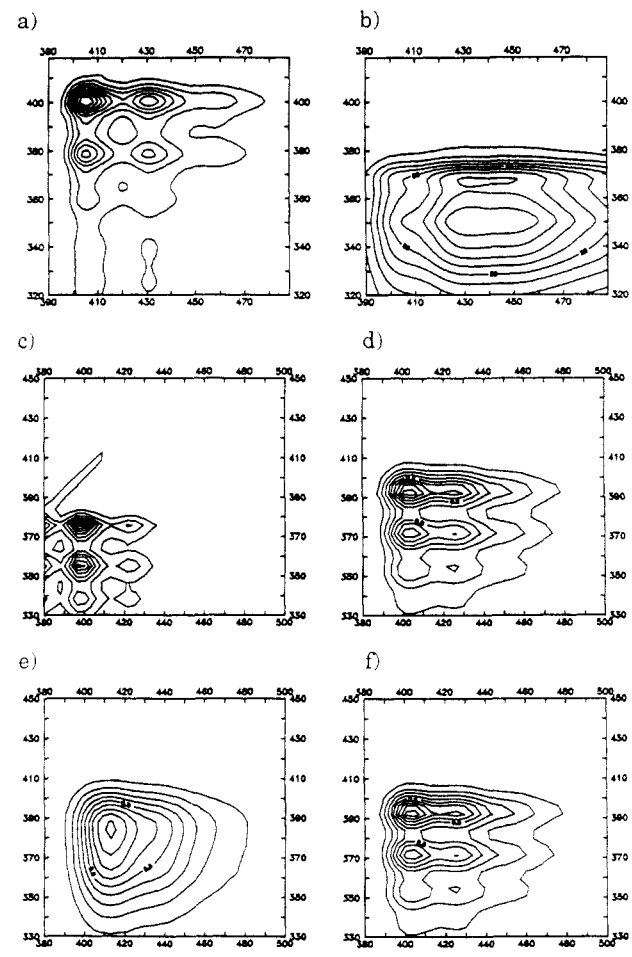

Figure 2. EEMs for three two-component systems studied: BkF (a) and BbF (b); ANT (c) and DPA (d); and TPP (d) and DPA (f). The vertical axis is excitation wavelength (in nanometers) and the horizontal axis is emission wavelength (in nanometers).

Table II. UMCs of Extracted Component Spectra of DPA and ANT from Multiway Analysis Using 5-, 10-, 20-, 40-, and 80-MHz PREEMs and Steady-State WCV Analysis

	extracted EEM 1		extracted EEM 2	
	ANT	DPA	ANT	DPA
1:1 DPA–ANT				
PREEM multiway	0.3460	0.9621	0.9090	0.6208
steady-state WCV	0.3328	0.9664	0.9690	0.5762
5:1 DPA–ANT				
PREEM multiway	0.3440	0.9592	0.8500	0.6864
steady-state WCV	0.3459	0.9708	0.9298	0.6142
1:5 DPA–ANT				
PREEM multiway	0.3385	0.9570	0.9060	0.6322
steady-state WCV	0.3432	0.9691	0.9871	0.5508
10:1 DPA–ANT				
PREEM multiway	0.3562	0.9661	0.2381	0.1647
steady-state WCV	0.3580	0.9740	0.8283	0.6540
1:10 DPA–ANT				
PREEM multiway	0.3991	0.9760	0.9254	0.5885
steady-state WCV	0.3357	0.9620	0.9986	0.5154

in the UMCs for spectra resolved from this system in Table II. While neither steady-state WCV analysis nor five-frequency multiway analysis do an excellent job resolving the system, in nearly all cases resolution is superior for the steady-state analysis. In this system, we appear to have reached the limits of lifetime resolution between two components.

Table III. UMCs of Extracted Component Spectra of DPA and TPP from Multiway Analysis Using 10-, 20-, 40-, 80-, 120-, and 160-MHz PREEMs and Steady-State WCV Analysis

	extracted EEM 1		extracted EEM 2	
	DPA	TPP	DPA	TPP
1:1 DPA–TPP				
PREEM multiway	0.8976	0.9814	0.9898	0.8713
steady-state WCV	0.6698	0.9001	0.9884	0.9630
5:1 DPA–TPP				
PREEM multiway	0.8687	0.9853	0.9657	0.8955
steady-state WCV	0.6867	0.9075	0.9992	0.9275
1:5 DPA–TPP				
PREEM multiway	0.9025	0.9786	0.8971	0.7568
steady-state WCV	0.9550	0.9926	0.6831	0.9070
10:1 DPA–TPP				
PREEM multiway	0.9211	0.9842	0.9611	0.8749
steady-state WCV	0.8231	0.8729	0.9947	0.9428
1:10 DPA–TPP				
PREEM multiway	0.9051	0.9815	0.6131	0.8181
steady-state WCV	0.9451	0.9958	0.7152	0.9238

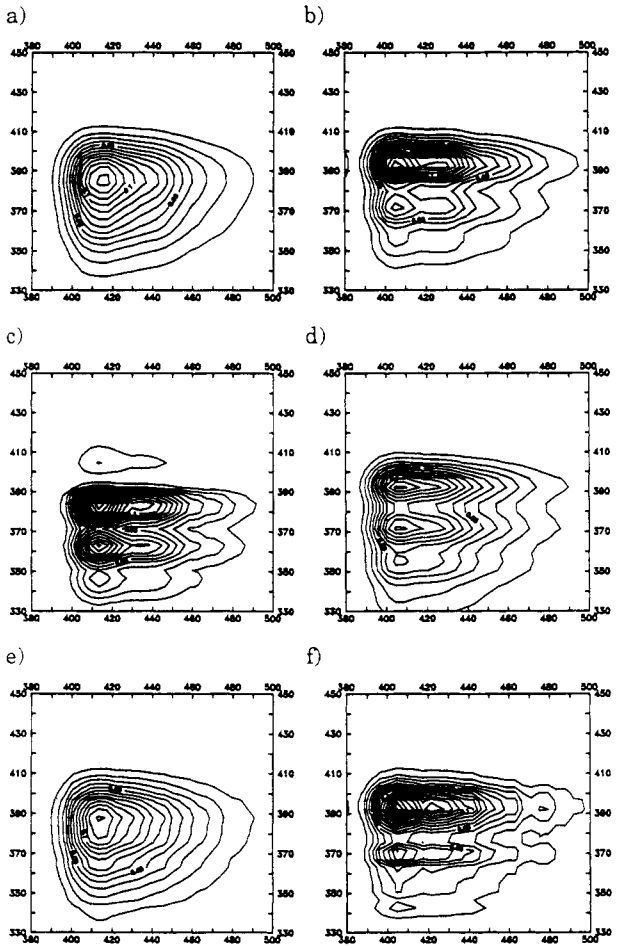

Figure 3. EEMs for extracted components 1 and 2: (a) and (b) six-frequency (10, 20, 40, 80, 120, and 160 MHz) multiway analysis of 1:1 DPA–TPP; (c) and (d) WCV steady-state analysis of 1:1 DPA–TPP; (e) and (f) WCV 120-MHz analysis of 1:1 DPA–TPP. The vertical axis is excitation wavelength (in nanometers) and the horizontal axis is emission wavelength (in nanometers).

DPA and TPP. This system appears to be at once easier and more difficult to resolve than DPA and ANT, in that the individual component spectra are much more highly overlapping but the lifetime difference is greater. While the absolute lifetime difference between ANT and TPP is small, the relative difference is sufficient to improve the resolution of the system, as is illustrated by the results in Table III. At every intensity ratio (with the exception of 1:10 DPA–TPP, where neither WCV or multiway work), resolution with a six-frequency multiway analysis is superior to that from the steady-state WCV analysis. Although some EEMs extracted

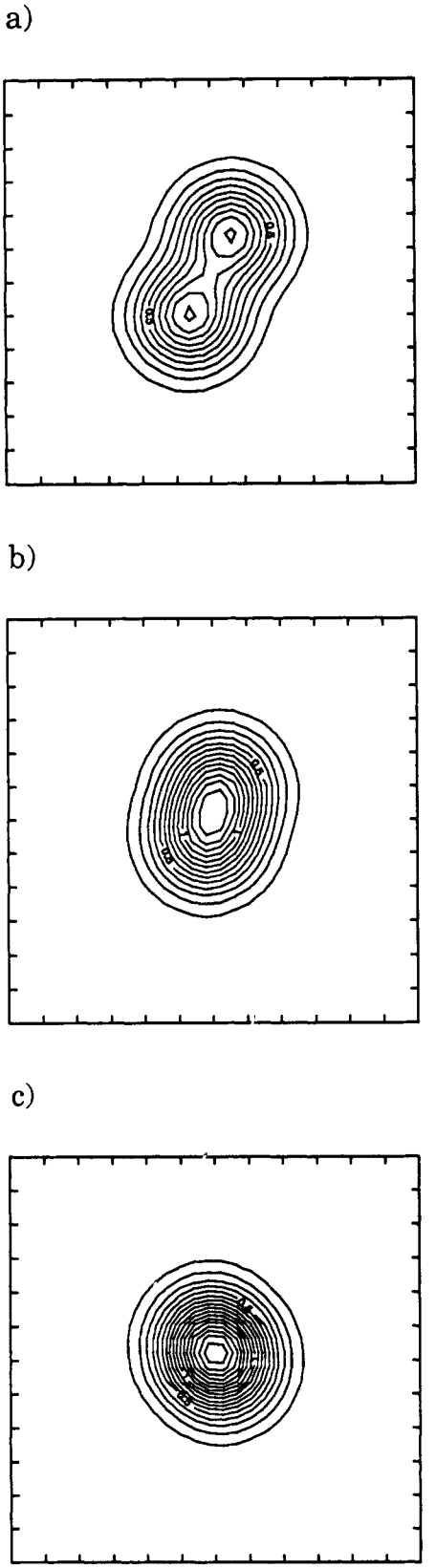

Figure 4. EEMs for simulated spectra: (a) Smix4, (b) Smix5, and (c) Smix6.

Table IV. UMCs of Extracted Component Spectra of DPA and TPP from Multiway Analysis and WCV Analysis

	extracted EEM 1		extracted EEM 2	
freqs, MHz	DPA	TPP	DPA	TPP
1:5 DPA–TPP				
PREEM Multiway				
10, 20, 40, 80, 120, 160	0.9025	0.9786	0.8971	0.7568
20, 40, 80, 120, 160	0.9019	0.9789	0.9108	0.7880
40, 80, 120, 160	0.9006	0.9818	0.8926	0.7922
80, 120, 160	0.9110	0.9803	0.1859	0.3977
20, 80, 160	0.9012	0.9777	0.9290	0.8156
80, 120	0.9146	0.9808	0.7358	0.8531
80, 160	0.9075	0.9765	0.8115	0.7104
40, 120	0.9026	0.9838	0.7074	0.5222
40, 160	0.9000	0.9776	0.9170	0.8195
WCV				
steady state	0.9550	0.9926	0.6831	0.9070
10	0.8882	0.9666	0.9193	0.8171
20	0.7094	0.8978	0.8224	0.7002
40	0.8915	0.9799	0.9215	0.8260
80	0.7538	0.9235	0.8956	0.8900
120	0.8850	0.9625	0.9130	0.9614
160	0.8628	0.9314	0.4933	0.5319

with steady-state WCV analysis correlate higher with a particular component (such as extracted EEM #2 with DPA at 1:1 DPA–TPP), in each of these cases the extracted EEM correlates too highly with the other component, indicating incomplete resolution; in addition, the correlation of the other corresponding extracted EEM with the other component is too low.

Figure 3 shows the resolved component spectra of DPA and TPP obtained from the WCV and multiway analyses. The six-frequency, multiway-resolved EEMs (a and b) correlate highly to the standard EEMs for both components (Figure 2, parts e and f), whereas the EEM extracted by steady-state WCV most closely corresponding to TPP (c) clearly has too much DPA character in it. The WCV analysis of a PREEM collected at 120 MHz (e and f) is more successful; presumably the high modulation frequency enhances the short-lived TPP fluorescence enough for it to be well-resolved while leaving enough DPA contribution for a good resolution of that component. The DPA–TPP system is an example of the case in which good extraction of individual component spectra requires the extra resolving power of lifetime selectivity.

An example of the effect of varying the modulation frequencies and the number of frequencies used for both WCV and multiway analysis is shown in Table IV for the 1:5 DPA–TPP solution. While small improvements in correlation can be obtained with a particular combination of modulation frequencies, the effect is not very great for these solutions. In addition, while optimization of the modulation frequency for the WCV-PREEM analysis of the 1:5 DPA–TPP solution can provide better resolution than that obtained with steady-state WCV, the results are only slightly better than multiway analysis, which is a more general approach that does not require optimization for particular components.

Computer Simulations. Computer-simulated spectra with varying degrees of spectral overlap, noise, and lifetime difference permitted a more systematic investigation of the limits of resolution for the different analysis techniques. The spectra for the three most overlapping cases are shown in Figure 4. Six different degrees of spectral overlap were investigated. All of the analysis techniques were able to fully resolve the four cases with the least overlap. Simulated mixtures of the remaining two, Smix5 (UMC = 0.5066) and Smix6 (UMC = 0.8173) were studied in greatest detail. One conclusion from the simulations that confirms an observation made above for the DPA and TPP system is that omitting particular frequencies from a multiway analysis does not generally improve resolution, although in some instances an optimal combination of frequencies can be found that does significantly improve the results. Spectral shapes of the individual components were also varied and did not appear to have a consistent effect upon quality of resolution.

Table V shows the mean UMCs and corresponding standard deviations for WCV steady-state and multiway PREEM analyses of Smix5 and Smix6 at two noise levels. Both approaches start to fail for Smix5 at 0.25 noise and for Smix6 at both noise levels; for Smix5 at 0.10 noise, multiway analysis at a lifetime difference of 2 and 3 ns is more successful than steady-state WCV by a statistically significant margin.

CONCLUSIONS

The results indicate that the chemometric resolution of individual component spectra from two-component solutions can be improved by the addition of fluorescence lifetime as a third dimension of selectivity, using multiway analysis techniques. We also demonstrate a case (the DPA–ANT system) for which the lifetime difference between two components is insufficient to aid resolution. Multiway analysis

Table V. Average of UMCs of Extracted Component Spectra (Simulated) for 10 Replicates of Multiway Analysis of 10-, 20-, 40-, 80-, 120-, and 160-MHz PREEMs and of WCV Analysis of Steady-State EEMs[a]

	extracted EEM 1		extracted EEM 2	
	std A	std B	std A	std B
Smix5, 0.10 Noise				
steady-state WCV	0.9555 (0.0223)	0.6138 (0.0765)	0.5834 (0.0773)	0.9565 (0.0241)
PREEM multiway				
2 & 3 ns	0.9840 (0.0127)	0.5490 (0.1199)	0.4750 (0.0848)	0.9864 (0.0087)
2 & 2.5 ns	0.8847 (0.2505)	0.5128 (0.2162)	0.4209 (0.1966)	0.9649 (0.0426)
2 & 2.25 ns	0.7811 (0.2090)	0.4058 (0.3102)	0.6209 (0.2004)	0.8166 (0.2781)
Smix5, 0.25 Noise				
steady-state WCV	0.8074 (0.0560)	0.06564 (0.0926)	0.6449 (0.0774)	0.7957 (0.0748)
PREEM multiway				
2 & 3 ns	0.881 (0.0369)	0.8150 (0.0805)	0.2456 (0.1523)	0.5167 (0.3221)
Smix6, 0.10 Noise				
steady-state WCV	0.9254 (0.0437)	0.8058 (0.0731)	0.8318 (0.0611)	0.9414 (0.0364)
PREEM multiway				
2 & 3 ns	0.8305 (0.2899)	0.7096 (0.2662)	0.6721 (0.2256)	0.8930 (0.1354)
Smix6, 0.25 Noise				
steady-state WCV	0.8465 (0.1054)	0.7781 (0.0808)	0.6986 (0.1213)	0.8007 (0.0823)

[a] Standard Deviations are in Parentheses.

of dynamic spectral data is particularly interesting in its potential application to exploratory, nondestructive analysis of fluorescent mixtures, since no assumptions regarding spectral shape or lifetime are necessary. We are currently exploring the application of frequency-domain fluorescence techniques to the analysis of more complex samples.

ACKNOWLEDGMENT

We appreciate the participation of Donald S. Burdick and Xin M. Tu of the Institute of Statistics and Decision Sciences and Department of Mathematics at Duke University in the data analysis.

LITERATURE CITED

(1) Warner, I. M. In *Comtemporary Topics in Analytical and Clinical Chemistry*; Hercules, D. M., Hieftje, G. M., Snyder, L. R., Evenson, M. A., Eds.; Plenum Press: New York, 1982; Vol. 4.
(2) Russell, M. D.; Gouterman, M. *Spectrochim. Acta* **1988**, *44A*, 857.
(3) Russell, M. D.; Gouterman, M. *Spectrochim. Acta* **1988**, *44A*, 863.
(4) Russell, M. D.; Gouterman, M.; Van Zee, J. A. *Spectrochim. Acta* **1988**, *44A*, 873.
(5) Millican, D. W.; McGown, L. B. *Anal. Chem.* **1989**, *61*, 580.
(6) Burdick, D. S.; Tu, X. M.; McGown, L. B.; Millican, D. W. *J. Chemom.* **1990**, *4*, 15.
(7) Lakowicz, J. R. *Principles of Fluorescence Spectroscopy*; Plenum Press: New York, 1983.
(8) Mattheis, J. R.; Mitchell, G. W.; Spencer, R. D. In *New Directions in Molecular Luminescence*; Eastwood, D., Ed.; ASTM: Philadelphia, PA, 1983.
(9) McGown, L. B.; Millican, D. W. *Appl. Spectrosc.* **1988**, *42*, 1084.
(10) Burdick, D. S.; Tu, X. M. *J. Chemom.* **1989**, *3*, 431.

RECEIVED for review May 11, 1990. Accepted July 19, 1990. This work was supported by the United States Department of Energy (Grant NO. DE-FG05-88ER13931).

Transient Infrared Transmission Spectroscopy

Roger W. Jones* and John F. McClelland

Center for Advanced Technology Development, Iowa State University, Ames, Iowa 50011

Transient infrared transmission spectroscopy is a new method that can acquire analytically useful transmission spectra from moving, optically thick solids. No sample preparation is required. The spectra are of sufficient quality for accurate quantitative compositional analysis. The method works by the creation of a thin, short-lived, chilled layer at the sample surface. Blackbody-like thermal emission from the bulk of the sample is selectively absorbed as it passes through the chilled layer, so the transmission spectrum of the layer is superimposed on the observed thermal emission. Spectra of polycarbonate, beeswax, and copolymers of methyl and butyl methacrylate are presented. Compositional analysis of the methacrylate copolymers with a standard error of prediction of only 0.87 mol % is demonstrated.

INTRODUCTION

The analysis of solids by infrared spectroscopy has long been problematic because of the high optical density of most solids at infrared wavelengths, but methods have been developed to cope with the difficulties. On the other hand, if the analysis must also be done in real time on moving sample material, such as on an industrial process line, it may not be possible by any method. Conventional transmission spectroscopy requires dilution or physical thinning to lower the optical density of the sample, but this precludes real-time analysis, is labor intensive, and destroys sample integrity. Diffuse reflectance can examine moving solids in real time without sample preparation but is largely limited to powders and places limits on the optical scattering, optical absorption, and morphological properties of the sample material (*1*, *2*). Photoacoustic spectroscopy can be applied to solids with a wide range of morphologies and without sample preparation, but the sample material must be acoustically isolated, limiting it to near real-time analysis and precluding on-line applications (*1*, *3*). Conventional emission spectroscopy is limited by optical density the same way transmission spectroscopy is. High optical density induces self-absorption and obscures the spectrum, so conventional emission spectroscopy is limited to optically thin samples (*4*).

Recently a new method called transient infrared emission spectroscopy (TIRES), which can analyze in real time optically thick solids in motion, has been under development (*5*–*7*). In TIRES an optically thin surface layer of the sample is rapidly heated for an instant and thermal emission from this layer is collected before it thickens and cools by thermal diffusion. This reduces self-absorption to levels that allow quantitative spectra and results to be obtained. Although TIRES works well on a wide variety of materials, it does rely on surface heating and on sensing thermal emission. Accordingly, the hotter the surface is, or more precisely, the greater the thermal gradient between the surface and the bulk is, the better. This means TIRES may not be applicable to certain thermally sensitive materials or to streams of hot material, such as often occur in industrial process settings. Transient infrared spectroscopy in general, however, only requires a sharp, near-surface thermal gradient to produce an optically thin surface layer not in thermal equilibrium with the sample bulk. The surface may be either hotter or *colder* than the bulk. We introduce in this paper a technique called transient infrared transmission spectroscopy (TIRTS) which uses a chilled surface layer.

In TIRTS, a jet of cold gas or some other cold source rapidly cools the surface of a moving stream of solid sample material within the field of view of a spectrometer. This produces an optically thin, chilled layer at the sample surface within the field of view. The layer thickens and warms by thermal diffusion, but as it does so it is also carried out of the field of view by the sample motion. As a result, the chilled layer within the spectrometer field of view remains thin. The uncooled, optically thick bulk of the sample acts as the infrared source of TIRTS since it behaves as a blackbody infrared-emission source. The thermal emission from the bulk must pass through the chilled surface layer to reach the spectrom-

*To whom correspondence should be addressed.

0003-2700/90/0362-2247$02.50/0